LA-UR-14-28189 (Accepted Manuscript)

Electronic structure of U2PtC2 and U2RhC2

Ronning, Filip
Zhu, Jianxin

To be published in: Journal of Physics: Conference Series, Vol.592, p.012037, 2015.

DOI to publisher's version: 10.1088/1742-6596/592/1/012037

Permalink to record: http://permalink.lanl.gov/object/view?what=info:lanl-repo/lareport/LA-UR-14-28189

Electronic structure of U_2PtC_2 and U_2RhC_2

F. Ronning and J.-X. Zhu

Los Alamos National Lab, Los Alamos, NM, 87544, USA

E-mail: fronning@lanl.gov

Abstract. We present density functional theory calculations within the generalized gradient approximation of U_2RhC_2 and U_2PtC_2. We find the calculated density of states are significantly less than that measured by specific heat indicating the need for electronic correlations. The mass enhancement found for U_2PtC_2 is $m^*/m_{band} \approx 4$.

1. Introduction

In 1969, Bernd Matthias *et. al.* discovered superconductivity in U_2PtC_2 at 1.47 K [1]. Meissner later identified U_2PtC_2, with a Sommerfeld coefficient of 75 mJ/mol-U K^2, as an "intermediate heavy fermion" [2]. In this case "intermediate" is relative to the Sommerfeld coefficients of UPt_3 and U_6Fe; the former is a well known unconventional superconductor, while the latter is typically believed to be a conventional superconductor. Heavy fermion behavior in U_2PtC_2 is also observed by optical spectroscopy and point contact tunneling measurements [3–5]. This then begs the question of whether or not the superconducting state in U_2PtC_2 is unconventional. Unusual power laws in the superconducting state can be observed in specific heat [6], NMR [7], and penetration depth [8]. Furthermore, the NMR work shows no Knight shift anomaly upon entering the superconducting state, which is suggestive of spin triplet superconductivity. In addition, the modified Koringa behavior observed in the normal state of U_2PtC_2 indicates the presence of strong ferromagnetic correlations. However, attempts to find the nearby ferromagnetic state have thus far been elusive. Pressure suppresses the superconducting transition and reduces the amount of inelastic scattering, which implies that pressure drives U_2PtC_2 away from any magnetic instability [9]. While the isostructural compounds U_2MC_2 with M = Os or Ru are paramagnetic, those with M = Rh and Ir are antiferromagnetic [10]. For U_2RhC_2 and U_2IrC_2 the antiferromagnetism appears to be more itinerant in nature [11; 12]. The doping series $U_2(Pt,Rh)C_2$ and $U_2(Pt,Ir)C_2$ identify an antiferromagnetic quantum critical point [11–13] whose fluctuations appear to compete with superconductivity rather than enhance it. In the case of U_2RhC_2 a spin flop transition is observed at small magnetic fields which may suggest proximity to a competing ferromagnetic state hinted at by the spin lattice relaxation rate measurements in U_2PtC_2 mentioned above.

To gain some insight into the physics of U_2PtC_2 we performed density functional theory (DFT) calculations on U_2PtC_2 and U_2RhC_2. We find that the density of states are 17 and 32 states/eV-f.u. for U_2PtC_2 and U_2RhC_2, respectively. Compared to the experimental value from heat capacity measurements this indicates that U_2PtC_2 has a mass enhancement $m^*/m_{band} \approx 4$. The electronic structure for both U_2PtC_2 and U_2RhC_2 have rather complex Fermi surfaces.

2. Methods

We performed DFT calculations using the generalized gradient approximation as implemented in the WIEN2K code [14] with the exchange correlation potential of Perdew, Burke, and Ernzerhof [15]. Spin orbit coupling was included in a second variational scheme. U_2MC_2 (M = Pt, Rh) forms in the body centered tetragonal structure with the Na_2HgO_2 structure type. The fractional atomic coordinates are (0,0,0) for the transition metal site, (0,0,z_C) for the carbon site, and (0,0,z_U) for the uranium site. All sites are fully occupied. We used the lattice parameters of a = 3.5287 Å and c = 12.5672 Å for U_2PtC_2[16] and a = 3.464 Å and c = 12.513 Å for U_2RhC_2[17]. The internal atomic positions z_C = 0.168, and z_U = 0.355 were assumed to be identical to that of the isotypic compound U_2IrC_2[18]. The muffin tin radii for both calculations were 1.11 Å, 0.98 Å, and 1.24 Å for the transition metal, carbon and uranium sites, respectively. In both cases the magnetic solution is lowest in energy. However, as U_2PtC_2 is paramagnetic and the primary compound of interest, all calculations presented here are constrained to be non-magnetic.

3. Results and Discussion

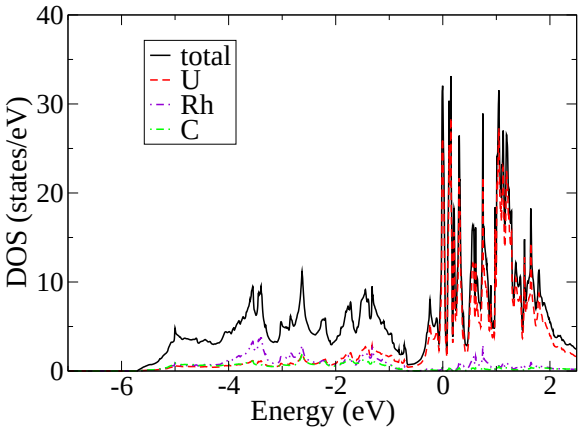

Figure 1. Total and partial density of states as a function of energy for U_2RhC_2.

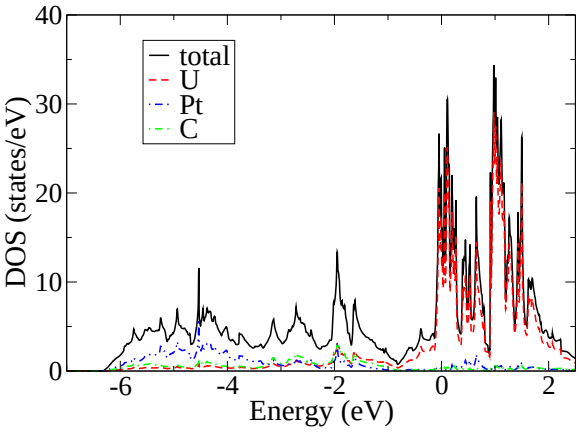

Figure 2. Total and partial density of states as a function of energy for U_2PtC_2.

Figures 1 and 2 present the partial density of states for both U_2PtC_2 and U_2RhC_2. In U_2RhC_2 the nearly filled transition metal d-band begins $\sim$ 6 eV below the Fermi energy. The Pt 5d band of U_2PtC_2 is slightly broader in energy relative to the 4d band of Rh, as expected. In both cases the states at the Fermi energy are dominantly of uranium 5f-character. The correspondence of features between the transition metal, uranium, and carbon partial density of states indicates good hybridization between all the elements. The density of states at the Fermi energy $N(E_F)$ = 17 and 32 states/eV-f.u. for U_2PtC_2 and U_2RhC_2, respectively, which corresponds to a Sommerfeld coefficient for the T linear term in the heat capacity of 20 and 38 mJ/mol-U K^2, respectively (note that the formula unit contains 2 uranium atoms). Thus, the mass enhancement compared with the band calculation for U_2PtC_2 is $m^*/m_{band} \approx 4$. Clearly, electronic correlations not captured by the present calculation must be present in U_2PtC_2. The experimental Sommerfeld coefficient in U_2RhC_2 is 80 mJ/mol-U K^2 within the magnetically ordered state[11]. The magnetic entropy recovered at T_N is less than 1/2 of R ln 2, where R is the Gas constant, and the saturated moment is only 0.3 μ_B/U. Furthermore, the resistivity data shows a Cr-like anomaly which is consistent with the notion that parts of the Fermi surface are gapped out upon entering the Néel state. Consequently, the value of 80 mJ/mol-UK^2 represents

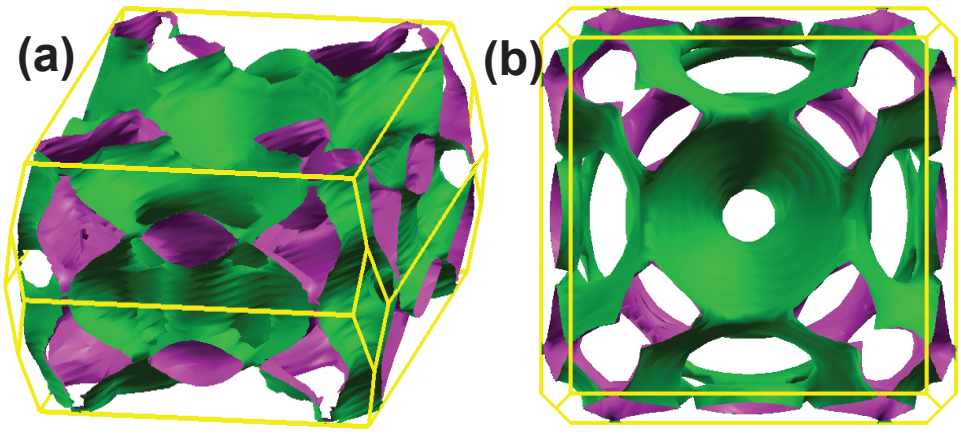

Figure 3. The Fermi Surface of U_2RhC_2. The Fermi surface displayed in panel (a) is projected down along the c-axis in panel (b).

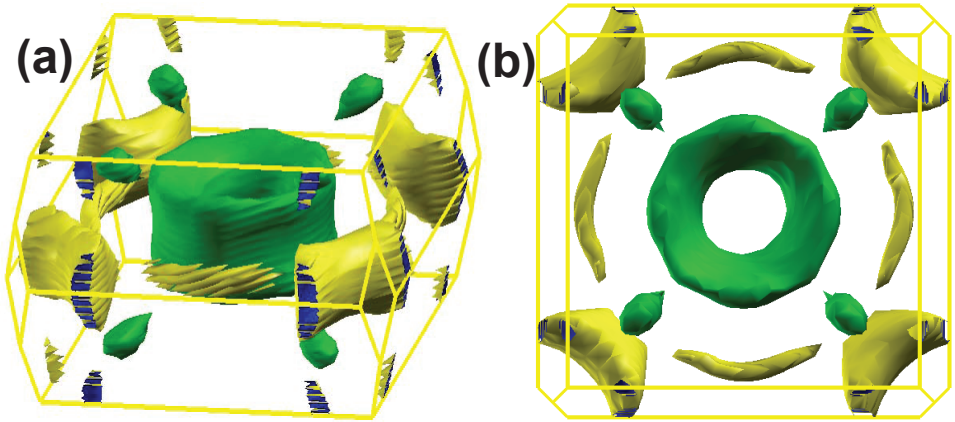

Figure 4. The Fermi Surface of U_2PtC_2. The Fermi surface displayed in panel (a) is projected down along the c-axis in panel (b).

a conservative lower bound for the effective mass of the paramagnetic state of U_2RhC_2, and hence we can say that m^*/m_{band} is more than 2 in the Rh analog. In our view, the larger density of states in the Rh analog relative to U_2PtC_2 encourages the formation of a magnetically ordered state.

An itinerant picture for the antiferromagnetic order in U_2RhC_2 would suggest that Fermi surface nesting is relevant in the case of U_2RhC_2. Thus, we computed the Fermi surface as shown in Fig. 3. There is one band that crosses the Fermi energy in U_2RhC_2, and is rather complex. There is no clear nesting feature found in the Fermi surface of U_2RhC_2 shown in Fig. 3. One possibility is that the Fermi surface including electronic correlations is significantly different from that shown in Fig. 3.

In going from U_2RhC_2 to U_2PtC_2, the lattice expands and, in addition, one electron is added to the Fermi sea. One expects, due to the lattice expansion, the hybridization to the $5f$-orbitals to weaken. However, the dominant change to the Fermi surface is a result of the additional electron. The complex Fermi surface in U_2RhC_2 shrinks and a new band now also crosses the Fermi energy (see Fig. 4). It is interesting that this is a very small electron pocket that extends over a large portion of the Brillouin zone (blue/yellow surface in Fig. 4). It is intriguing to speculate whether this pocket could enhance the susceptbility at small momentum transfer and

thereby be responsible for the ferromagnetic correlations observed in the normal state by NMR [7].

4. Conclusion

We have presented first-principles calculations of the electronic structure of U_2RhC_2 and U_2PtC_2. The fact that magnetic ordering is observed in U_2RhC_2 and not in U_2PtC_2 could be attributed to the larger density of states of the former. This is a consequence of the band filling in U_2RhC_2. Thus, we would anticipate that magnetic order could also be found in $U_2(Os_{0.5},Pt_{0.5})C_2$ and $U_2(Ru_{0.5},Pt_{0.5})C_2$. Consistent with this idea, we note that U_2OsC_2 is non-magnetic down to 1.3 K with a Sommerfeld coefficient of the heat capacity of only 20 mJ/mol-U K^2 [13]. With regards to superconductivity in U_2PtC_2, we note that the isostructural compound Th_2NiC_2 is also superconducting at $T_c = 8$ K [19]. Computation shows this system to be likely electron-phonon mediated by a dominant C-Ni-C stretching mode [20; 21]. It is possible that a similar C-Pt-C stretching mode mediates superconductivity in U_2PtC_2. However, this can not easily explain the anomalous superconducting properties observed by specific heat, NMR and μSR measurements [6–8], and clearly electronic correlations play a role in the uranium based systems, as we observe a mass enhancement of approximately 4 in U_2PtC_2. More work is needed to elucidate the nature of superconductivity in U_2PtC_2.

Acknowledgments

We thank N. Wakeham, A. Mounce, Ni Ni, J.D. Thompson, E. D. Bauer, R. Movshovich, M. Janoschek, J. Smith, G. Stewart, G. Meisner, and Z. Fisk for useful discussions. Work by F.R. was performed under the auspices of the Department of Energy, Office of Basic Energy Sciences, Division of Materials Science and Engineering, while J.-X.Z. was supported by the LANL LDRD program.

References

[1] Matthias B T, Chu C W, Corenzwit E and Wohlleben D 1969 *Proceedings of the National Academy of Sciences of the United States of America* **64** 459–461

[2] Meisner G, Giorgi A, Lawson A, Stewart G, Willis J, Wire M and Smith J 1984 *Physical Review Letters* **53** 1829–1832

[3] Marabelli F and Wachter P 1990 *Solid State Communications* **74** 1075–1078

[4] Moser M, Wachter P, Franse J, Meisner G and E W 1986 *Journal of Magnetism and Magnetic Materials* **54-57** 373–374

[5] Naidyuk Y G, Yanson I K Chubov P N, Kirzhner V M, Panova G K and Alekseeva Z M 1988 *Sov. Phys.-Sol. State* **30** 1343

[6] Movshovich R *et. al.* 2014 unpublished

[7] Mounce A M, Yasuoka H, Koutroulakis G, Ni N, Bauer E D, Ronning F and Thompson J D 2014 (*Preprint* 1408.1969) URL `http://arxiv.org/abs/1408.1969`

[8] Wu W D, Keren A, Le L P, Luke G M, Sternlieb B J, Uemura Y J, Sato N, Komatsubara T and Meisner G P 1994 *Hyperfine Interactions* **85** 425–430

[9] Thompson J and Meisner G 1985 *Physica B* **130** 168–170

[10] Ebel T, Wachtmann K and Jeitschko W 1996 *Solid state communications* **97** 815–819

[11] Wakeham N, Ni N, Bauer E D, Thompson J D, Tegtmeier E and Ronning F 2015 *Phys. Rev. B* **91**(2) 024408

[12] Kang M, Wakeham N, Ni N, Bauer E, Kim J and Ronning F 2014 unpublished

[13] Killer U, Kim W W, Mielke A, Fraunberger G, Rieger J J, Scheidt E W and Stewart G R 1994 *Phys. Rev. B* **49** 1188–1191

[14] P. Blaha et al., An Augmented Plane Wave + Local Orbitals Program for Calculating Crystal Properties (K. Schwarz, Tech. Universitat Wien, Austria, 2001).

[15] Perdew J P, Burke K and Ernzerhof M 1996 *Phys. Rev. Lett.* **77**(18) 3865–3868

[16] Haines H R and Potter P E 1969 *Nature* **221** 1238

[17] Holleck H 1968 *J. Nuc. Matt.* **28** 339

[18] Bowman A L, Arnold G P, Krikorian N H and Zachariasen W H 1971 *Acta Crystallographica Section B* **27** 1067–1068

[19] Machado A J S, Grant T and Fisk Z 2012 *Superconductor Science and Technology* **25** 045010

[20] Quan Y and Pickett W E 2013 *Phys. Rev. B* **88** 014501

[21] Shein I and Ivanovskii A 2013 *Journal of Alloys and Compounds* **551** 338 – 342